GEOMETRY AND MATERIAL OPTIMIZATION IN SOLENOID VALVE MAGNETS USING SIMULATION AMBIENT

Derryck Antoniuk de Souza, Thais Barcella Marchese

Robert Bosch Ltda

E-mails: Derryck.Souza@br.bosch.com, Thais.Marchese@br.bosch.com

ABSTRACT

Many diesel engines use valves actuated by electromagnets in the fuel system in order to control the injection. Earlier models of these systems have pumps controlled by solenoid valves, in this case with a magnet with E shaped lamination and armature connected to the valve. From the beginning of the project, it was used the theory of transformers and the core was designed with a lamination of stacked steel sheets. In the later diesel systems, the concept of the valve and the core material were changed. Considering that, it was defined a study for the replacement of the core material, considering the development of the new materials and process available in the market. Since the component has a construction complexity, it was decided to perform a pre-analysis using a simulation ambient (ANSYS Maxwell) in order to validate the material change and possible design optimization. The material choice was made considering the magnetic response to the PWM current generation and frequency, which affects directly the core losses. The main goal of this study is to determine a material commercially available and that behaves on the same way as the current component, since no change in the performance is allowed. After the definition of material and geometry, samples were ordered for test bench validation.

1. INTRODUCTION

In this paper, electromagnetic simulations were performed in order to study the influence of the core material change on a solenoid valve. It was proposed a change from a laminated E shaped core (series stator) for a bulk sintered material (new stator). It is important to remark that the coil and the armature considered for the series and the new stator are the same. This study was made firstly with a mathematical model, without considering losses, for an initial approach of the material response. Then, a second step was carried out using finite elements simulation with ANSYS Maxwell, considering eddy current losses. With the preliminary results, it was possible to define an optimized geometry in order to meet the valve response time, since the function and compatibility of the components must be preserved.

2. MOTIVATION

Considering the theory of electromagnetism and transformers, it is well known that the usage of laminated core for these applications are the best and cheapest choice, considering the correlation of cost and performance. There are many options, going through simple ferrite materials and more sophisticate ones, as Silicon and Cobalt alloys. The main issue with

laminated components is the manufacturing complexity for some geometries and its limitations when considering mechanical strength. In order to overcome these manufacturing limitations, it was necessary to change the core from laminated to a solid material.

3. SYSTEM DESCRIPTION

The electromagnet, subject of this study, also called stator, is applied in Diesel engines in order to control the beginning and ending of the injection period. It is a component of the Unit Pump and have the design function described in the Figure 1.

The construction of the valve basically consists in a stator creating a magnetic force to attract the armature. The armature is connected to the high pressure valve, that when closed, isolates the low pressure side to the high pressure side, enabling the fluid to be compressed and generating pressure for the injection at the desired time [1].

The stator has the core laminated and an E shape geometry. The winding is connected to the ECU (Electronic Control Unit) and receive voltage in PWM DC function in order to generate a current profile. The electric function is described in the Figure 2 [1].
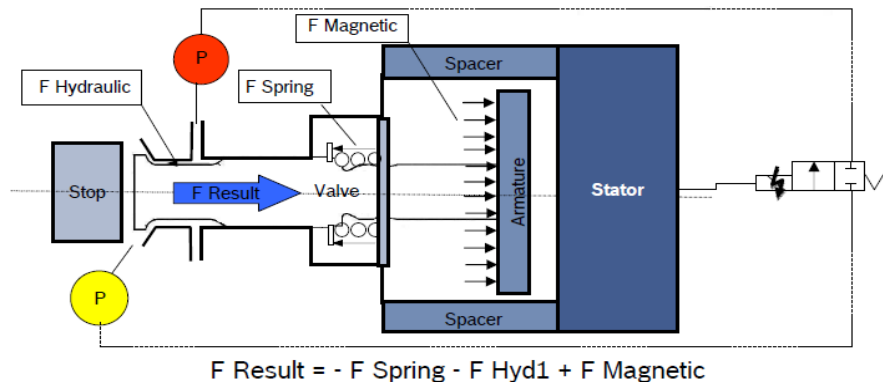
F Result = - F Spring - F Hyd1 + F Magnetic
Figure 1 - Unit Pump Function
Source: Robert Bosch
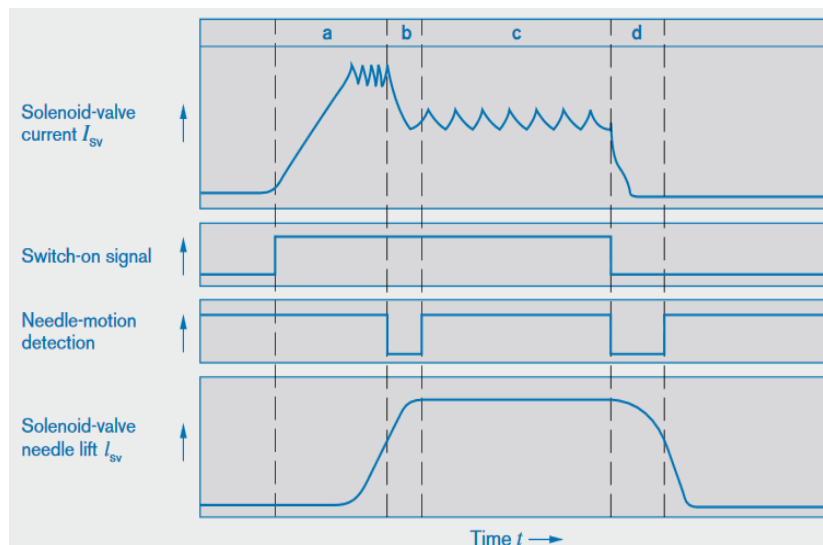
**Figure 2 - Electric Function**
Source: Robert Bosch

4. ELECTROMAGNETIC ANALYSIS

The first step is to analyze theoretically, what is the magnetic response of the current and the proposed materials. In order to do this analysis, the reluctance model of the component must be built to allow the calculation of magnetic force in the air gap. In this case, a magnetic force will be calculated without the losses, as an initial approach. This analysis is valid only for comparison of material characteristics and geometry.

4.1. Reluctance model

The reluctance model is the first step for the system analysis, where the lamination, air gap and armature geometries and materials permeability are taken into account. The sections considered are shown in Figure 3.
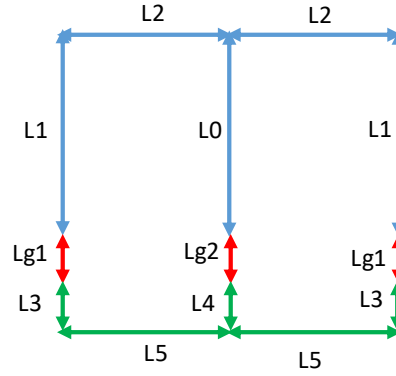
Figure 3 - Reluctance Model

For the force calculation, first it is necessary to determine the reluctance (R) of the system, calculating each one of the sections shown in Figure 3 with the Equation 1.

$$R = \sum_{i=1}^{i=n} \frac{l_i}{\mu_i A_i}$$

Eq. 1

where l is the section length, μ is the material relative permeability for the corresponding section and A is the cross sectional area [2].

It is important to notice that the values Lg_1, Lg_2 and Lg_3 represent the air gaps and the length of these sections change for each step of movement, affecting the final force. The next step is to determine the magnetic flux in the system. The sum of the reluctance is used in the Equation 2.

$$\Phi = \frac{NI}{R}$$

Eq. 2

where N is the number of turns of the winding and I is the applied current [2].

For the magnetic force calculation, the force at the air gap (F_{gap}) is considered, since this is the area relevant for the analysis. For the calculation, the whole magnetic flux value (Φ) is used within the cross-section area of the air gap. It is calculated for each

section and summed up for the final value. Also the permeability of the air gap is considered:

$$F_{gap} = \frac{B^2 A}{2\mu_0} = \frac{\Phi^2}{2A\mu_0}$$

Eq. 3

Where B is the magnetic flux density and μ_o is the free space permeability [2].

4.1.1. *Results from the reluctance model*

Based on the equations shown in the section 4.1, the theoretical magnetic force for the new stator, without considering any losses, was calculated. It is important to remark that a simplified version of the geometries were considered in the calculations, especially the armature geometry, that originally has some holes that result on a smaller air gap area, and in this case was considered as a solid component.

First it was made a calculation considering the current geometry and material, and then with a new design and material proposal. In this step, it was not considered any loss in the core, so the results represent an ideal situation. The maximum magnetic force reached in a condition where the air gap is 0.1 mm and the current is 14 A is approximately 250 N for the series stator and 300 N for the new stator, as shown in the Figure 4 and in the Figure 5.
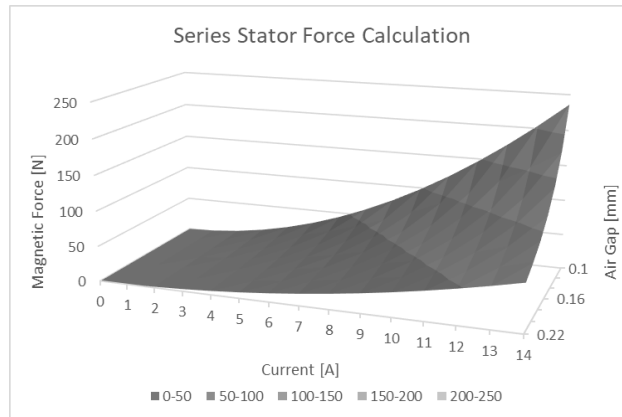
**Figure 4 - Reluctance Model Results – Series Stator**
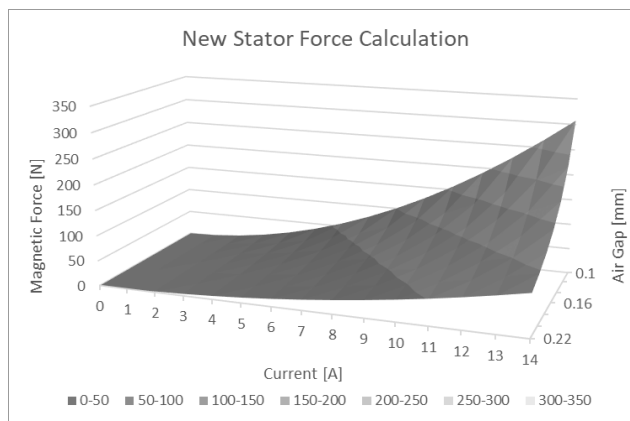
Figure 5 - Reluctance Model Results – New Stator

The properties of the core material were taken from the data sheet provided by the supplier and the armature material data were available from measurements.

4.2. Magnetic Losses

After an initial analysis of the magnetic force, it is important to consider the losses. The current profile resultant the DC PWM voltage signal, generate important losses in two moments: while there is a high variance of the density flux B and while there is a high switching frequency (Figure 6).
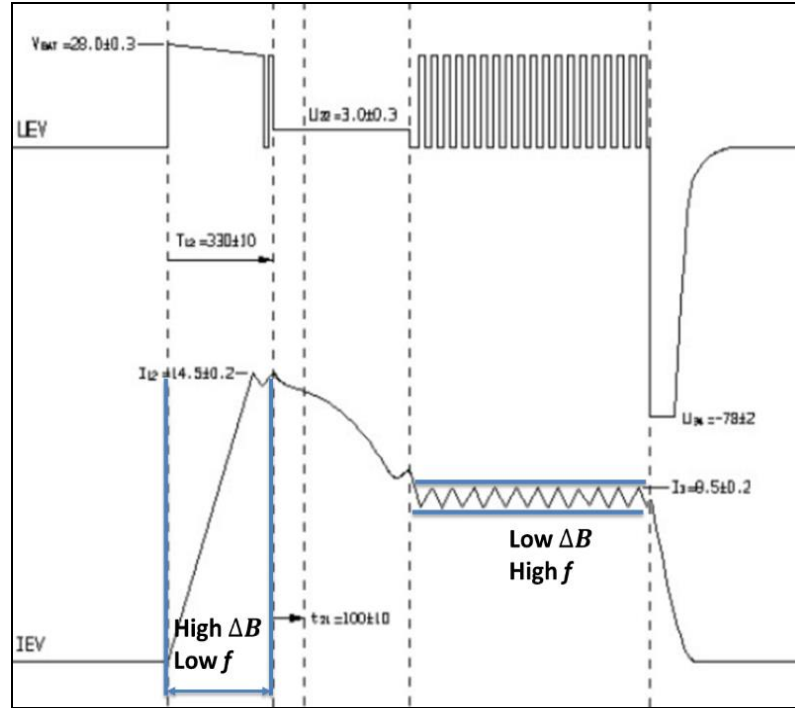
Figure 6 - Voltage and Current Profiles
Source: Robert Bosch

The losses are commonly evaluated in power losses (P_s). It can be expressed by the sum of Eddy Current (P_E), Hysteresis (P_H) and other losses (P_{EX}), as shown in Equations 4 and 5.

$$P_s = P_E + P_H + P_{EX}$$ Eq. 4

$$P_s = \frac{1}{\rho}\frac{1}{T}\int_0^T H\frac{dB}{dt}dt$$ Eq. 5

where ρ is the material density, T is the time period. and H is the magnetic field strength [3].

The other losses (P_{EX}) will not be considered in this study, since they can be generated by many sources, as induced heat and external magnetic fields.
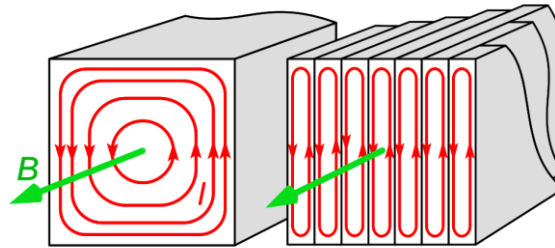
4.2.1. *Eddy current losses*

Since the materials of this study are magnetic materials and have a good electric conductivity, according to the Lenz's Law, the magnetic fields within the core will induce currents, called Eddy Currents, parallel to the flux. This flux opposes the desired magnetic field, imposing the total flux generated. The Eddy Current losses are directly proportional to the frequency and field density. This can be estimated by the Steinmetz equation, shown in Equation 6.

$$P_E = \frac{\pi^2 \sigma d^2}{6\rho} (\hat{B} f)^2$$

Eq. 6

where σ is the material conductivity, ρ the density of the material, d is the core width, $\hat{B}$ is the filed amplitude, at a frequency f.[4]

Another factor that influences the eddy current is the material width, as d represents the in Equation 6. The thinner the geometry, the lower is the eddy current generated (Figure 7). Many transformers and precision magnets use a stack of thin metal sheets, insulated from each other, which prevents the eddy current to flux from an area to the other. This reduces considerably the energy loss in the core. Also the use of sintered material can cause the same effect, since each grain formed is isolated from each other, normally by a resin. The only penalty in the sintered materials is the loss of field density, what impacts directly to the final magnetic force. [4]

**Figure 7 - Eddy Current Losses**
Source: [5]

4.2.2. *Hysteresis losses*

For the hysteresis loss analysis is important to understand the theory of magnetization, where there is the alignment of the atomic dipoles when a ferromagnetic material receives an external magnetic flux, for example the field that a current induces in a copper wire in a winding. This magnetization occurs until the magnetic saturation of the material is reached. Due to the material properties and frequency (f), the demagnetization of the material does not occurs at the same line as the magnetization due to residual magnetism, also called remanence. This effect also causes a power loss (P_H), which influences directly the final magnetic force, what can be estimated by the Equation 7.

$$P_H = K_H f \hat{B}^n \qquad \text{Eq. 7}$$

where K_H is the hysteresis coefficient, that need to be measured, and n is the Steinmetz exponent and varies from 1.5 to 2.5. [4].

In our study application, the modulation on the current profile (Figure 6) makes the material work only on the first quadrant of the magnetization curve. The modulation makes the current oscillate between two defined levels, and, therefore, the magnetic field strength (H), which is given in A.m, also oscillates between two values, creating what is called "minor loop" on the magnetization curve. This behavior is represented in the Figure 8. [6]
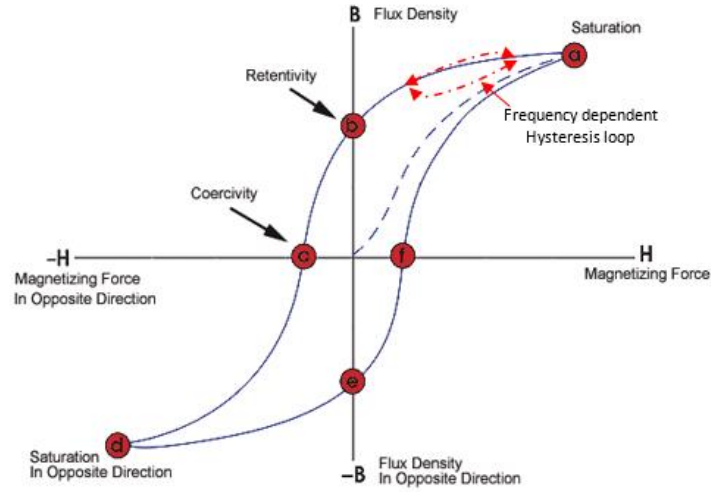
Figure 8 - Hysteresis Curve
Source: [5]

5. SIMULATION

After the theoretical study that led to the design definition, some simulations were performed in order to confirm the results. Using the 3D model of the new stator (Figure 9), the materials characteristics and the real current profile from the application (Figure 10) as input, the simulations were performed using the transient solver of the software ANSYS Maxwell.
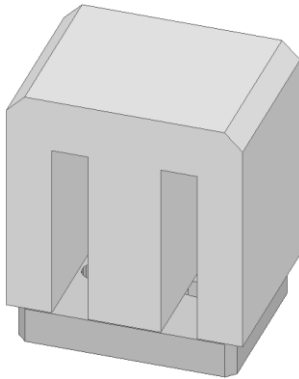


Figure 9 – New Stator 3D Model
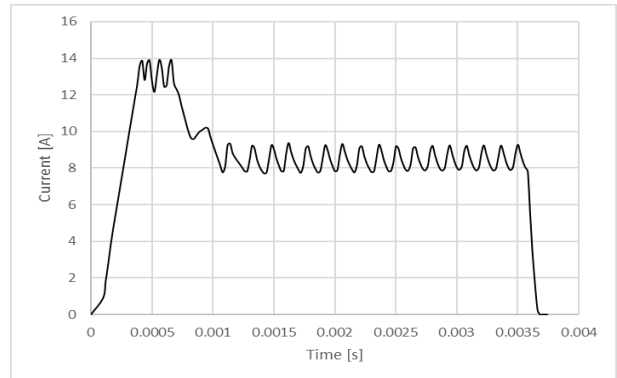
Figure 10 - Current Profile

5.1. Simulation Setup

After importing the geometry, the core and armature materials were defined based on their BH curves and bulk conductivities. The characteristics of the core material were taken from the data sheet provided by the supplier and the armature material data were available from previous measurements. As the core loss curves were not available for the armature material, the only parameters considered on the losses calculation were the bulk conductivities, which are used for the eddy current losses computation.

In order to reduce the computational time, the coil was modeled on a simplified way, only by a box representing its volume. The volume occupied by the coil model is approximately the same as the one occupied by the real coil. A section was made on the coil geometry in order to define the current direction and the number of turns.

Since the adaptive meshing is not available for the transient solver and the strategy used for the eddy losses calculation requires a refined mesh in order to have good results, the mesh was built first on the magnetostatic solver and then exported to the transient solver [7]. The mesh has a skin depth layer calculated based on the material permeability, bulk conductivity and applied frequency. The resulting mesh is shown in the Figures 11, 12, 13 and 14. The skin depth refinement can be seen clearly in Figures 13 and 14.
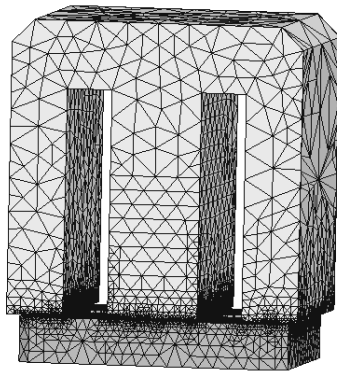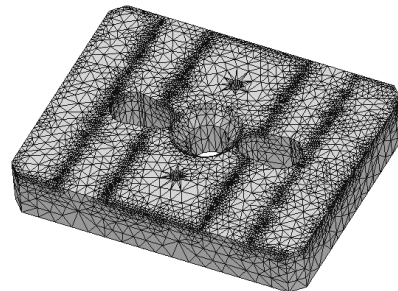

Figure 11 - Stator Mesh
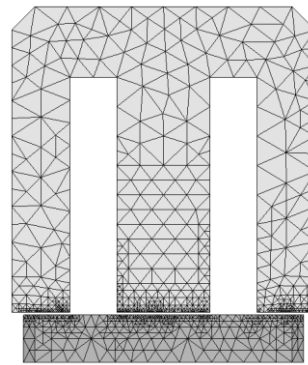
Figure 12 - Mesh - Frontal View
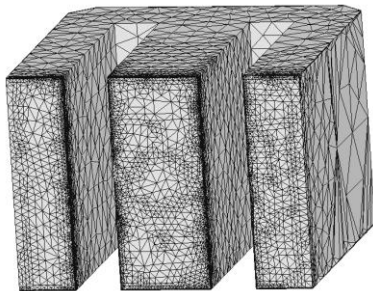
Figure 13 - Core Mesh - Bottom View

Figure 14 - Armature Mesh

5.2. Results

The evaluated results from this simulation were the magnetic force, the armature displacement and the eddy losses. In order to reduce the computational time, the current profile showed in Figure 10 was not applied completely, only the pull in level

(Figure 15), which is enough to evaluate the armature lift behavior, was considered. A simulation of the series stator performed previously was used as reference in order to compare the results and analyze the new stator behavior. Since no change on the component performance is allowed, the armature rise time, measured from the beginning of the energizing time to the moment when the armature reaches the maximum lift value, must not be higher than 1.1 ms. This value was taken from the component specification.
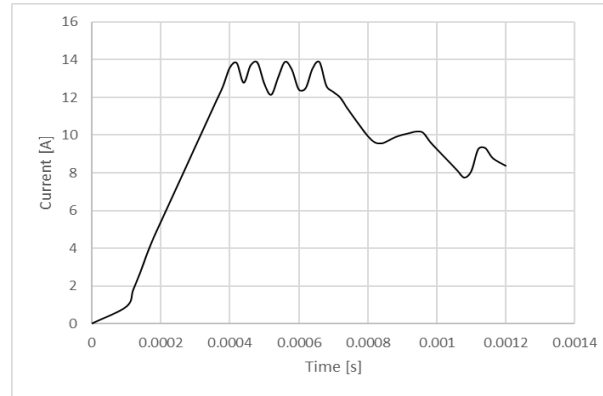

**Figure 15 - Current Profile - Pull in Level**

The simulation of the series stator (Figure 16) was performed using the same mesh and losses calculation strategies used for the new stator simulation, the differences between them are the core geometry and material and the coil volume. Also, is important to remark that the series stator core is laminated, therefore the losses values should be significantly lower when compared to the new stator results.
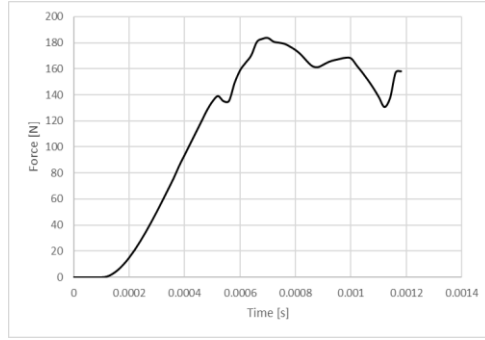
5.2.1. *Series stator*

The series stator simulation shows that the armature takes approximately 660 μs to reach the maximum displacement value (Figure 17). This result is within the specified time limit and is coherent when considering measurement values. Other evaluated parameters are the magnetic force (Figure 18), which reaches a maximum value of 183 N, and the losses (Figure 19), that reach up to 9 W.
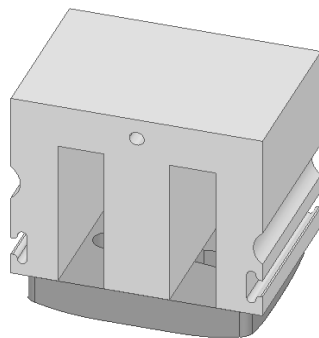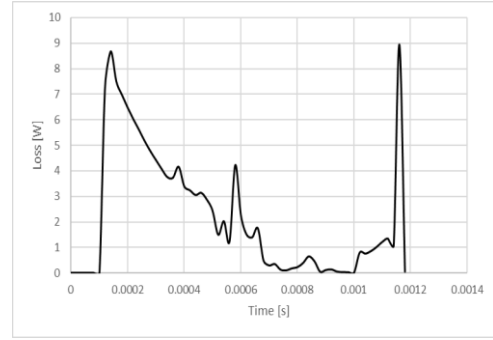

Figure 16 - Series Stator
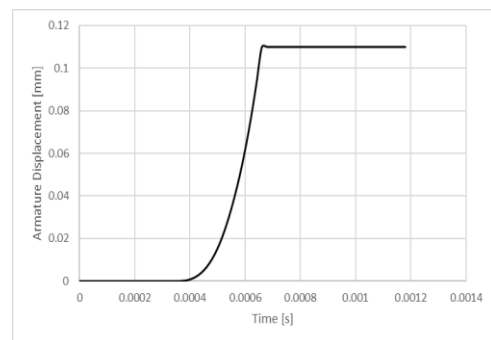
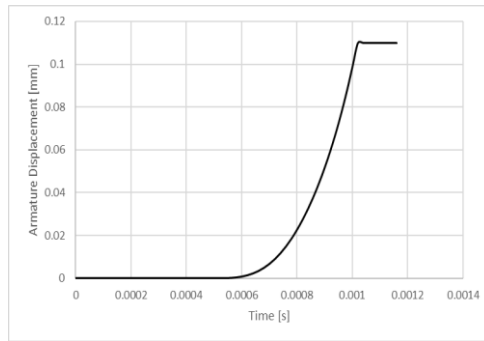**Figure 17 - Series Stator - Armature Displacement**

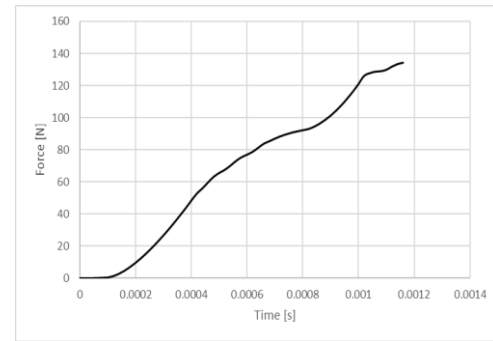**Figure 18 - Series Stator - Magnetic Force**

Figure 19 - Series Stator – Loss
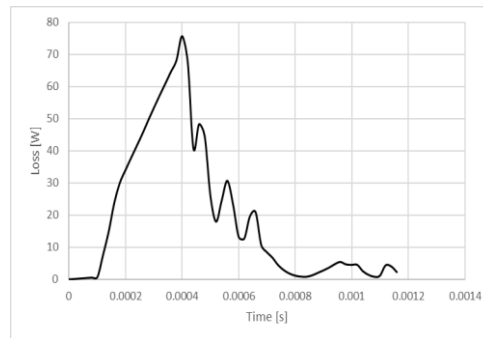
5.2.2. *New stator*

The results from the new stator simulation show that the armature takes 1 ms to reach the maximum lift value (Figure 20), which, even being bellow the specified limit of 1.1 ms, the time interval is significantly higher than the one achieved by the series stator. The magnetic force reaches a maximum value of 134 N (Figure 21) and the losses can reach values up to 75 W (Figure 22).

Figure 20 - New Stator - Armature Displacement

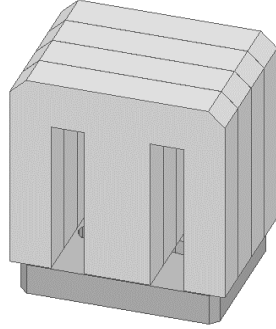**Figure 21 - New Stator - Magnetic Force**

Figure 22 - New Stator – Loss
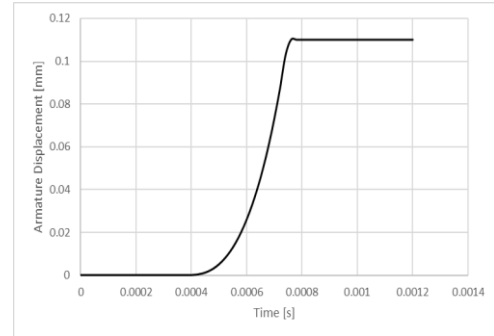
5.2.3. *New stator – modified core*

Even with the armature of the new stator taking a time within the specification to reach the maximum displacement value, a modification on the core geometry was studied in order to try to make this value closer to the series stator. This modification consisted on splitting the core on 4 parts, as shown in Figure 23,

and adding an isolation between them. As on a lamination, this geometry makes the eddy effects be lower than on a solid core.
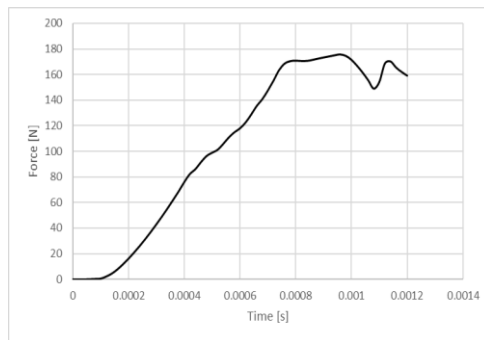
The results from the simulation of this modified core show that the armature takes 760 µs to reach the higher displacement limit (Figure 24), a value that is closer to the result from the series stator. The maximum magnetic force reached by this design is 175 N (Figure 25) and the losses can reach 68 W (**Figure 26**).
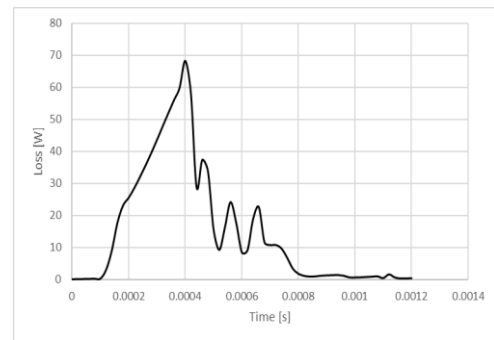

Figure 23 – New Stator Modified

**Figure 24 - New Stator Modified - Armature Displacement**

**Figure 25 - New Stator Modified - Magnetic Force**

Figure 26 - New Stator Modified – Loss

5.2.4. *Comparative*

Analyzing the results shown in the sections 5.2.1, 5.2.2 and 5.2.3 and comparing them, it is possible to see that the results from the simulations of the new stator with the modified core are much closer to the results from the series design. The comparative results shown in the Figure 27, armature displacement, and Figure 28, magnetic force, make clear that the modified design has a higher probability of keeping the original performance behavior as the series design. The losses, shown in Figure 29, are much higher on the modified new stator than on the series stator, but these losses are compensated by other characteristics of the core material, as the permeability and saturation, what allow the component to achieve high magnetic forces.
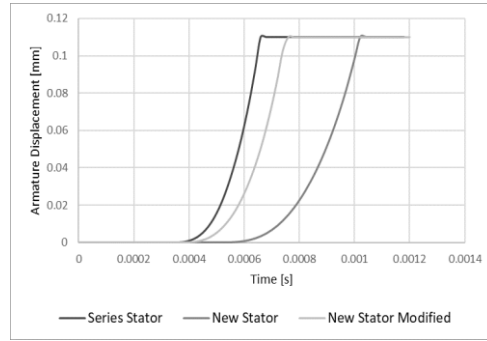
Figure 27 - Comparative - Armature Displacement
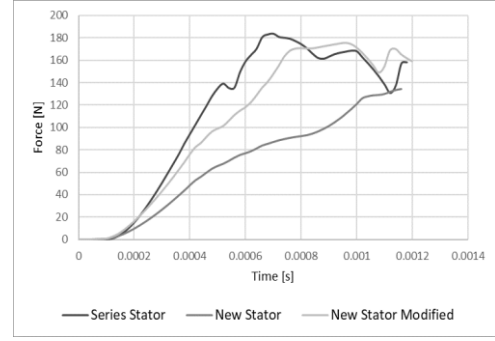
Figure 28 - Comparative - Magnetic Force
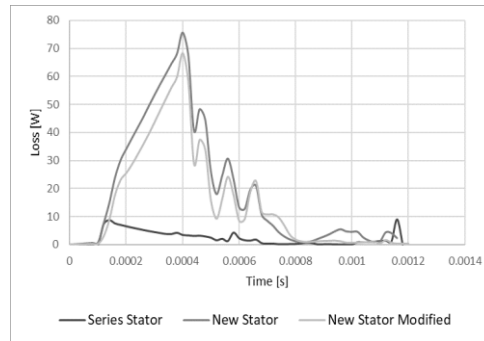
Figure 29 - Comparative – Loss

Comparing the simulated results for magnetic force from the series stator and the new stator with the calculated results showed in the section 4.1.1 it is possible to notice a significant difference between the maximum values. For a condition where the current is 14 A and the air gap is 0.1 mm, the theoretical calculations show that the magnetic force for the series stator is approximately 250 N and for the new stator, it is 300 N, while the simulations reached 183 N for the series stator and 134 N for the new stator.

The differences between the calculated and the simulated magnetic force values can be explained by the consideration of the losses on the simulations and also by the simplified geometry considered on the theoretical analysis. The differences on the values of the new stator are bigger than the one of the series stator because the losses are more significant.

CONCLUSION

For the theoretical calculations, it was verified that they could be used for estimation of force comparison with known geometries and losses. If the construction of the core is changed, for example from laminated to sintered, and the effect of losses are not known, the theoretical analysis can lead to results that do not represent well the reality.

Analyzing the FEM simulation for the series stator, it showed a good result compared to the known application data and rise time tolerances, so it can be used as reference. It is important to remark that the characterization of the core material was known from measured data that

were validated. For the new stator, the core material characterization was obtained from a supplier data sheet, and these properties can change after the machining process of the final component, therefore the simulation results must be validated with tests. For the simulation results analysis, the proposed design and material reached the tolerance of rise time, but also with a higher loss compared to the series design, which was expected since the material is not laminated.

Comparing the results from the theoretical calculations and the simulations was possible to see that are significant differences on the magnetic force. These differences can be explained by the fact that the losses were taken into account only on the simulations. As expected, the differences on the results are much higher on the new stator, since the losses due to eddy current are higher on solid cores.

It was studied a proposal for the high loss issue, where the core of the new stator was splitted in 4 parts, in order to reduce the sectional area for eddy current generation. The simulation showed a good improvement in the rise time in this case, giving a closer response to the series design.

In order to validate the simulation, the proposed material was acquired from two different suppliers and will be validated in functional samples. The idea is to assemble the components in a Unit Pump and mount in the test bench. Samples will be manufactured with the one-piece sintered core and with 4 core divisions.

It will be done a pump map, to the see the difference between the series component and the proposed one. With this test is possible to analyze the current profile generated with the PWM signal from the ECU, the shot-to-shot injection variance and the rise time (from the software point of view). From these results, we can define if it is feasible or not to replace the core material without any penalty to the function of the Unit Pump system.

REFERENCES

[1] KLINGEBIEL, M; DIETSCHE, K. **Diesel Fuel-Injection Systems - Unit Injector System and Unit Pump System.** Germany: Robert Bosch GmbH (2006).
 [2] CASTRO, Hélio F. **Experimental performance evaluation of magnetic actuator used in rotating machinery analysis**. Rio de Janeiro: J. Braz. Soc. Mech. Sci. & Eng v. 29, n. 1, p. 99-108, Mar. 2007.
[3] TACCA, H. E; SULLIVAN, C. R. **Extended Steinmetz equation. Report of Postdoctoral Research.** 2002.
[4] CHEN, Y.; PILLAY, P. **An improved formula for lamination core loss calculations in machines operating with high frequency and high flux density excitation.** Conference Record of the 2002 IEEE Industry Applications Conference. 37th IAS Annual Meeting (Cat. No.02CH37344), 2, 759-766 vol.2. 2002.
[5] COLLINS, Danielle. **Hysteresis loss and eddy current loss: What's the difference?.** Available on: https://www.motioncontroltips.com/hysteresis-loss/. Accessed: May 2019.
[6] Prof P.Parthasaradhy; Dr S.V.Ranganayakulu. **Hysteresis and eddy current losses of magnetic material by Epstein frame method-novel approach.** The International Journal Of Engineering And Science (IJES). Pages 85-9. 2014.
[7] ANSYS Inc. **Maxwell Help**, Release 19.2, July, 2018